Eur. Phys. J. D **37**, 377–383 (2006)
DOI: 10.1140/epjd/e2005-00331-2

THE EUROPEAN PHYSICAL JOURNAL D

Positron and electron scattering from alkane molecules

Normal- and cyclo-octane

O. Sueoka[1], C. Makochekanwa[2,3,a], and M. Kimura[2]

[1] Faculty of Engineering, Yamaguchi University, Ube, Yamaguchi, 755-8611, Japan
[2] Graduate School of Sciences, Kyushu University, Fukuoka 812-8581, Japan
[3] Physics Department, Sophia University, Chiyoda-ku, Tokyo 102-8554, Japan

Received 27 August 2005 / Received in final form 29 September 2005
Published online 20 December 2005 – © EDP Sciences, Società Italiana di Fisica, Springer-Verlag 2005

Abstract. Total cross-sections (TCSs) for 0.2–1000 eV positrons and 0.4–1000 eV electrons colliding with normal-octane and cyclo-octane molecules have been studied using a relative measurement method. The TCS curves for positron and electron vary smoothly and compare well with other alkane molecules, in order of increasing carbon number. For positron scattering, weak humps at 1.5–2.5 eV for both normal- and cyclo-octane were observed. In the energy range lower than 2.2 eV, positron TCSs are roughly equal to or larger than electron TCSs. For electron scattering, a resonance peak at 8 eV and a shoulder at 25.0 eV were observed for both molecules. Over all the energy range, the TCS values for normal-octane are larger than those of cyclo-octane. The positron and electron TCS data for normal- and cyclo-octane molecules are briefly compared with those for normal- and cyclo-hexane.

PACS. 34.80.Bm Elastic scattering of electrons by atoms and molecules – 34.80.Dp Atomic excitation and ionization by electron impact – 36.10.Dr Positronium, muonium, muonic atoms and molecules

1 Introduction

Recent advances in the fields of micro and nanotechnology have been founded upon the technique of plasma etching of silicon devices. Key to this has been the ability to control atomic-order surface adsorption, diffusion and reactions in the etching processes. Hydrocarbons play an important role in high temperature plasmas in Tokamak fusion devices in plasma processing and many other fields [1]. On the other hand, fluorine-substituted hydrocarbons are not the less important also as they play significant roles as reactive agents in these plasma-assisted fabrication processes [2–4]. Our group has embarked on a systematic study of total scattering cross-sections (TCSs) from both hydrocarbons and perfluorocarbons (PFCs) with the hope of providing benchmark data for modeling of these industrial processes [5–7]. Whereas electron impact cross-sections are the needed parameters for modeling these processes, the comparative study between electron and positron scattering that we carry out here offers an effective tool for better understanding electron scattering phenomena. Notwithstanding, the recent developments of trap-based positron beams have gone a long way in enabling studies of positron-atom/molecule collision processes with improved resolution and intensities, i.e. enabling measurements of electronic and vibrational excitation cross-sections and annihilation rates [8]. Evidence of positronium (a bound state of an electron and positron) formation at energies below its literature threshold (defined as ionization energy *minus* 6.8 eV), and of dissociative positron attachment (DPA) have also began to come up, and thus renewed interest in positron-atom/molecule scattering [8]. As pointed out in reference [8], evidence on PDA is only just beginning to be studied but the first results indicate that hydrocarbons can effectively bind positrons while fluorocarbons do not, though for electron attachment the situation is reversed.

In this report we present the experimental results for positron and electron scattering from normal-octane and cyclo-octane molecules, within the same framework as in the previous study for normal- and cyclo-hexane molecules [7]. (Hereafter normal- and cyclo-, will be abbreviated n- and c-, respectively.) A detailed comparison of the electron and positron TCSs results for scattering from n- and c-octane is carried out with those for scattering from n- and c-hexane molecules. The experimental data for positron and electron TCS for n-octane (C_8H_{18}) and c-octane (C_8H_{16}) molecules presented here were corrected for forward scattering effect using a method similar to the one introduced and described in our previous studies [7,9,10].

To our knowledge, except for the data on the motion of thermal electrons in these molecules by Christophorou et al. [11], neither electron nor positron TCS data exist, either experimentally or theoretically, in literature on these molecules to compare the current results with.

[a] e-mail: casten@yamaguchi-u.ac.jp

2 Experimental procedure

2.1 Apparatus and projectiles

The experimental method used for studying the positron and electron TCSs for these molecules is the retarding potential time of flight (RP-TOF) approach similar to that used in our previous studies [12,13], and thus only a brief summary is given here. The same ^{22}Na radioisotope with an activity of 70 μCi was used as the source for both positron and electron beams. A set of conventional tungsten (W) ribbons, latter changed to the W-mesh type, was used for the positron beam moderator. The energy width of the positron beam is typically 2.3 eV at full width half maximum (FWHM). On the other hand, slow electron beams with an energy width of around 1.4 eV (FWHM), for electron scattering experiments, were produced as secondary electrons emerging from the same W moderator through multiple scattering. However, it must be pointed out though that this beam energy width is different from energy resolution of the RP-TOF experimental apparatus, which is less than 0.3 eV below 4 eV for both positron and electron impact, thus enabling discussions of structures observed even below 1 eV [14].

A retarding potential unit is included in the TOF apparatus as an energy selector for positron and electron beams. The retarding potential unit is placed in front of the beam detector, Ceratron, for eliminating the beam contribution from large energy loss inelastic scattering, and for decreasing elastically scattered and/or small energy loss, such as via vibrational and rotational excitation, contributions with reduced axial velocities. The specimen gases for both molecules were in liquid form and both had purities of 98%.

2.2 Total cross-section measurements

The TCS, or Q_t, values are obtained using the equation

$$Q_t = -\frac{1}{n\ell}\ln\left(\frac{I_g}{I_v}\right), \tag{1}$$

where n is gas density in the collision cell and ℓ is the effective length of the collision cell determined by normalizing our e^+–N_2 data to those of Hoffman et al. [15]. That is, the Q_t was determined relatively. I_g and I_v are the beam intensities in the gas run and vacuum run, respectively, and are determined from the raw TOF spectra using the method of Coleman et al. [16].

To confirm the independence of the effective length of the collision cell on gas pressure, TCS measurements for electron collision were performed for both n-C_8H_{18} and c-C_8H_{16} molecules. As shown in Figure 1, no pressure dependence of the Q_t values is observed.

2.3 Magnetic field and forward scattering correction

A magnetic field parallel to the flight path is applied using solenoid coils for beam transportation. The beam intensity strongly depends on the magnetic field strength, since the perpendicular component of the beam velocity to the flight path is magnetic field dependent. Besides, the exit aperture of the collision cell is very wide, being 3 mm in radius. According to these conditions of this apparatus, the detector ends up detecting some positron/electrons elastically scattered either with low energy losses or reduced axial velocity resulting from angular deflection, i.e. an effect called forward scattering. Thus, the raw data for measured TCSs are fairly affected by the forward scattering effect, i.e. for both positron and electron impact. The forward scattering effect in the measured cross-section, $Q_{measured}$, can be accounted for by the addition of the forward scattering cross-section, Q_f, to the measured cross-section as follows

$$Q_t = Q_{measured} + Q_f, \tag{2}$$

where Q_f is obtained by the method discussed already elsewhere [10]. Because there is no information on either positron or electron experimental and/or theoretical differential cross-section (DCS) data for both n- and c-octane, we made an attempt to derive synthesized DCSs for n-octane molecules using the DCS data for electron scattering from CH_4, C_2H_6 and n-propane (C_3H_8) [17–19], and c-propane DCSs [20] for c-octane. We also point out here that because there are no DCS data available for positron scattering, even for C_3H_8, the same synthesized electron DCS data were used for an attempt on the correction of positron TCSs too. The DCS data for the forward scattering correction was estimated using the following equation

$$\mathrm{DCS_{C8H18}} = \mathrm{DCS_{C3H8}}\frac{\mathrm{TCS_{C8H18}}}{\mathrm{TCS_{C3H8}}}. \tag{3}$$

These synthesized DCSs for n-octane were calculated using an idea based on the fact that (i) the electron-TCS data for alkane molecules vary monotonously with increasing carbon number as shown in the preliminary data (see

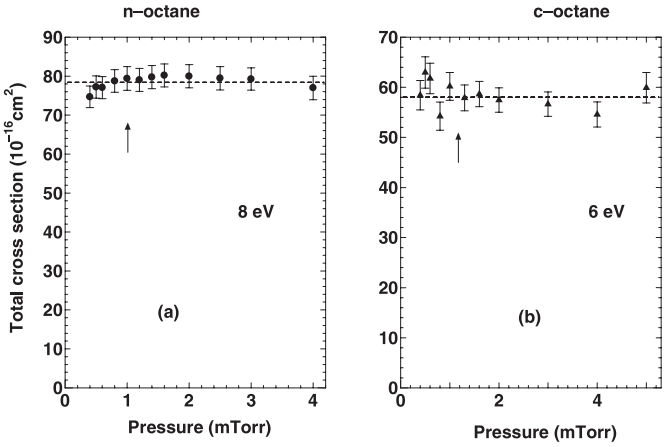

Fig. 1. TCSs for electron impact on (a) n-octane and (b) c-octane plotted against gas pressure for 8 eV and 6 eV impact energies, respectively. The beam intensity attenuation, I_g/I_v of 1/3, used for the conventional TCS measurements is shown by arrows. Error bars show the total uncertainties determined as explained in the text.

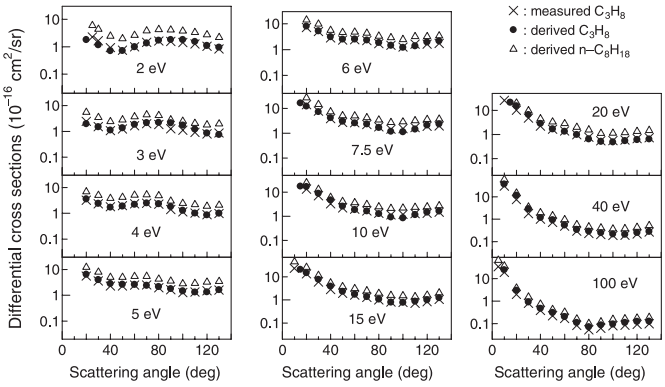

Fig. 2. Electron impact DCS: experimental results for C_3H_8 [19] and the C_3H_8 and n-C_8H_{18} results derived as explained in the text.

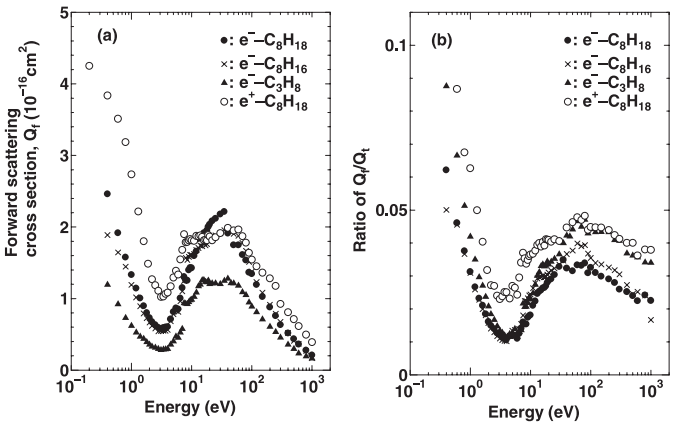

Fig. 3. (a) Forward scattering cross-section (Q_f) for: n-octane, c-octane, n-propane electron, and n-propane positron impact; and (b) the ratios of Q_f to TCS, Q_f/Q_t, for electron scattering from: n-octane, c-octane, n-propane electron, and n-propane positron scattering.

Fig. 2 of Ref. [7], and also our previous report [5]), (2) the electron-DCSs for CH_4 [17], C_2H_6 [18] and C_3H_8 [19] are not so significantly different, in terms of the energy dependence, except for the absolute values. The intensities of the DCSs are derived using the TCS data for n-propane and n-octane. The DCS values due to equation (3) at low angles and low energies were modified slightly using the following idea. From the values deduced from CH_4, C_2H_6 and C_3H_8 in the plot of the extrapolation data at zero angle versus the carbon number, the weak forward peaking shape of DCSs at low angles was deduced for octane. That is, a small modification of the value obtained from equation (3) was added to the DCS data at angles lower than 10 degrees and for energies lower than 4 eV. In order to check the credibility of this approximate method for deriving the unknown n-octane DCSs using equation (3), we carried out the same simulation to derive C_3H_8 DCSs from the measured C_2H_6 DCSs from reference [18], and the measured C_2H_6 [5,10] and C_3H_8 [10] TCSs. The results are shown in Figure 2. One sees that, despite the simplicity of the method we use here, we get both good qualitative and quantitative agreement between the measured C_3H_8 DCSs [19] and our derived C_3H_8 DCSs. Nevertheless, the derived DCSs tend to be slightly higher in magnitude than the measured values at 40 eV and above, albeit still within the reported errors of 20% [19]. Thus, we infer that our derived n-octane DCSs (also shown in Fig. 2) should be reliable for use here. Using the same assumption, the c-octane synthesized DCSs were derived using equation (3) and c-propane DCSs [20].

The forward scattering cross-sections, Q_f, for electron scattering by n- and c-octane in the present experiment are shown together with the data of C_3H_8 in Figure 3a, and also in the form of the ratios, Q_f/Q_t, in Figure 3b. These results are reasonable considering the derivation method used for the synthesized DCSs.

3 Results and discussion

The TCS values for positron scattering by n-octane (C_8H_{18}) and c-octane (C_8H_{16}) are presented in Table 1, while those for electron scattering by these molecules are given in Table 2. The errors shown are the total uncertainties estimated by addition of $\Delta n/n$, $\Delta l/l$ and $\Delta I/I$, where I refers to $\ln(I_g/I_v)$ in equation (1), and stands for statistical errors in the counting. The value of $\Delta I/I$ is around 2% for positron collisions and less than 1% for electron collisions. The error in the gas density n is almost certainly due to the accuracy of the pressure gauge (CMH4-M11 of Vacuum General, 0.03 mTorr); $\Delta n/n$ was around 0.5% depending on the collision gas pressure. The error due to normalization procedure for the determination of the effective length $\Delta l/l$ was estimated to be 2%.

Though we could not explicitly include the error rates involved in the forward scattering cross-section, Q_f, we estimate it to be an average 30% for both molecules for electron impact. This error is made up of errors in the original measured C_3H_8 (or cyclo-propane) DCSs, those due to the extrapolation of the measured C_3H_8 DCS to the experimentally inaccessible angles $<20°$ and $>120°$ and those arising from the derivation procedure of equation (3). It is expected that an additional uncertainty (which we assume to be not more than 15%) is introduced due to the use of electron impact DCS for positron TCS correction.

3.1 Positron scattering

The TCSs for positron scattering by n-octane (C_8H_{18}) and c-octane (C_8H_{16}) molecules were obtained using magnetic fields of 4.5 G and 9 G in the range 0.7–600 eV, and 9 G in the ranges 0.2–1.0 and 800–1000 eV. The magnetic field for electron scattering was 4.5 G over the whole energy range. The electron and positron scattering data were corrected for the forward scattering effect using the same artificial DCS data, taking into account the different magnetic field values for the different energy ranges, using the same method described above. That is, at any given energy, the positron DCS is different from that for electron impact because it is simulated using different TCSs and a

Table 1. Positron TCSs for C_8H_{18} and C_8H_{16} molecules after correction for the forward scattering effect. The numbers in parenthesis show the measured numerical values of the TCSs before the correction. Errors show total uncertainties derived as explained in the text.

E (eV)	C_8H_{18}	C_8H_{16}
0.2	38.1(33.9)±3.6	31.0(28.0)±5.1
0.4	33.7(29.9)±2.9	25.6(22.4)±2.8
0.6	40.3(36.8)±3.1	32.0(28.9)±3.7
0.8	45.9(42.8)±3.6	41.7 (38.8)±5.0
1.0	43.5(40.8)±2.4	40.4(37.6)±2.2
1.3	44.4(42.1)±2.4	43.0(40.7)±2.3
1.6	44.6(42.8)±2.3	44.9(43.0)±2.4
1.9	46.8(45.3)±2.4	44.5(43.0)±2.3
2.2	46.6(45.4)±2.3	42.6(41.3)±2.3
2.5	44.0(42.8)±2.3	44.0(42.8)±2.4
2.8	46.1(45.0)±2.6	43.7(42.7)±2.5
3.1	44.5(43.4)±2.5	43.2(42.2)±2.6
3.4	43.2(42.2)±2.3	44.5(43.6)±2.4
3.7	42.4(41.3)±2.4	44.1(43.1)±2.4
4.0	43.2(42.2)±2.3	42.5(41.5)±2.2
4.5	50.5(49.4)±2.6	42.6(41.6)±2.2
5.0	7.9(46.6)±2.6	43.0(41.8)±2.2
5.5	52.5(51.1)±2.7	46.0(44.8)±2.5
6.0	54.9(53.6)±3.2	45.2(44.0)±2.4
6.5	52.3(50.8)±2.8	45.6(44.2)±2.5
7.0	49.3(47.6)±2.7	48.6(47.0)±2.6
7.5	51.2(49.3)±2.7	47.0(45.5)±2.5
8.0	50.6(48.8)±2.7	45.5(43.9)±2.5
8.5	53.2(51.4)±2.7	46.8(45.2)±2.4
9.0	52.1(50.2)±2.7	46.6(44.9)±2.5
9.5	50.9(47.9)±2.8	46.3(44.7)±2.5
10	49.7(47.3)±2.9	46.0(44.3)±2.2
11	49.1(47.9)±2.5	45.8(44.1)±2.3
12	49.7(45.6)±2.7	43.4(41.7)±2.4
13	47.5(45.6)±2.5	43.4(41.7)±2.2
14	47.1(45.2)±2.6	42.0(40.3)±2.2
15	47.8(46.0)±2.6	41.4(39.7)±2.2
16	45.0(43.2)±2.6	42.0(40.4)±2.3
17	46.4(44.6)±2.5	42.3(40.7)±2.2
18	44.1(42.3)±2.6	41.0(39.4)±2.0
19	42.0(44.1)±2.6	39.2(37.5)±1.9
20	45.6(43.8)±2.8	39.5(37.8)±2.0
22	44.9(43.1)±2.3	41.8(40.0)±2.0
25	45.2(43.3)±2.8	40.9(39.1)±2.4
30	47.1(45.2)±2.6	40.6(38.8)±2.1
40	44.4(42.5)±2.4	41.1(39.1)±2.2
50	42.1(40.2)±2.2	38.4(36.5)±2.1
60	41.1(39.1)±2.2	38.3(36.4)±2.2
70	39.8(38.0)±2.2	36.3(34.5)±2.4
80	36.9(35.1)±2.1	35.6(33.8)±2.5
90	37.2(35.6)±2.1	33.6(32.0)±2.3
100	34.5(32.9)±2.1	31.4(29.9)±2.2
120	32.5(31.0)±2.0	30.4(28.9)±2.0
150	30.5(29.1)±2.0	29.4(28.0)±2.1
200	29.2(27.9)±2.0	24.2(23.0)±1.8
250	27.8(26.6)±2.1	23.5(22.4)±1.5
300	22.4(21.5)±1.5	21.1(20.1)±1.6
400	20.2(19.4)±1.1	19.8(19.0)±1.2
500	17.8(17.1)±1.2	17.0(16.3)±1.3
600	17.0(16.4)±1.0	14.5(13.9)±1.0
800	13.1(12.6)±0.6	12.5(12.1)±0.5
1000	10.3(9.9)±0.6	11.0(10.7)±0.5

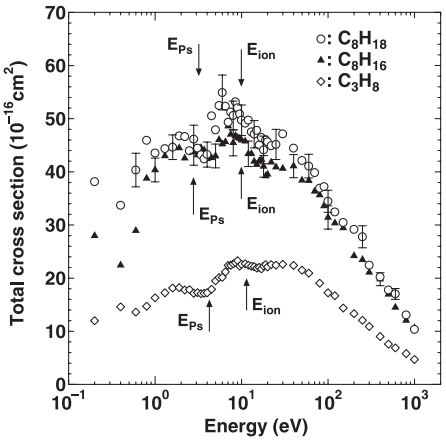

Fig. 4. TCSs for positron scattering from n-octane, c-octane and normal-propane molecules. Arrows indicate thresholds of Ps formation, $E_{\rm Ps}$, and ionization, E_{ion}.

different magnetic field strength. The TCS data for both 4.5 G and 9 G measurements were found to be consistent after the forward scattering correction.

The TCS data for positron scattering by n- and c-octane are presented in Figure 4, together with those for n-propane for comparison. Both TCSs show a peak at 1.5–2.5 eV, a feature that is observed for all alkanes from C_3H_8 and larger. This peak, being below the threshold for positronium formation, could be an indicator of some positron-in-molecule or resonance process [5]. For n-octane, the peak at around 6 eV is more pronounced than that for c-octane, which is rather flat. The structures at 4–12 eV should be due to a combination of positronium formation, electronic excitation and ionization channels. The origin of the shoulder at around 30–40 eV is not clear, though it could be attributed to impact ionization. However, the physics of the scattering resulting in this shoulder could also possibly have everything to do with valley at about 20 eV than the 30–40 eV shoulder. The magnitudes of the n-octane TCSs are 5–18% greater than those for c-octane at 5–50 eV. This difference is similar to that in the electron impact. Therefore, though the general shapes in the positron-TCSs for these two molecules are similar, it is apparent that there are many different features, when examined in greater detail, which are manifestations of the isomer effect.

For comparison of the cross-section data of octane with those of our recently studied hexane [7], the ratios of n-octane/n-hexane and c-octane/c-hexane have been

Table 2. Electron TCSs for C_8H_{18} and C_8H_{16} molecules after correction for the forward scattering effect. The numbers in parenthesis show the measured numerical values of the TCSs before the correction. Errors show total uncertainties derived as explained in the text.

E (eV)	C_8H_{18}	C_8H_{16}	E (eV)	C_8H_{18}	C_8H_{16}
0.4	39.6(37.1)±1.9	39.6 (37.7) ±1.9	13	74.5(72.7)±2.7	58.4(56.7)±2.2
0.6	41.6(39.7)±1.7	37.7 (36.1)±1.6	14	73.7(71.9)±2.8	58.8(57.0)±2.3
0.8	42.0(40.4)±1.6	39.4 (37.3)±1.5	15	73.4(71.6)±2.8	58.0(56.3)±2.2
1.0	42.6(41.3)±1.5	38.5 (38.0)±1.4	16	72.8(70.8)±2.8	59.0(57.2)±2.4
1.2	43.0(41.8)±1.6	39.2 (38.8)±1.4	17	72.4(70.5)±2.7	58.9(57.1)±2.3
1.4	43.3(42.3)±1.6	39.2 (38.8)±1.4	18	72.5(70.5)±2.8	59.2(57.4)±2.4
1.6	42.6(41.7)±1.6	39.8 (39.6)±1.9	19	71.6(69.6)±2.7	59.4(57.6)±2.3
1.8	43.3(42.5)±1.7	40.2 (40.5)±1.5	20	71.2(69.1)±2.8	58.9(57.1)±2.4
2.0	45.3(44.6)±1.7	42.3 (41.8)±1.6	22	71.7(69.6)±2.7	59.0(57.1)±2.3
2.2	45.2(44.6)±1.6	44. (043.3)±1.6	25	69.7(67.6)±2.7	58.3(56.4)±2.4
2.5	45.4(44.7)±1.7	45.2 (44.8)±1.7	30	66.3(64.2)±2.7	57.1(55.2)±2.4
2.8	47.0(46.4)±1.8	46.2(45.7)±1.8	35	63.5(61.3)±2.4	56.4(54.5)±2.4
3.1	47.5(46.9)±1.9	49.7 (49.1)±1.9	40	59.2(57.3)±2.2	54.1(52.1)±2.3
3.4	52.4(51.8)±2.0	52.0 (51.4)±2.0	50	55.4(53.7)±2.2	50.6(58.4)±2.1
3.7	54.7(54.1)±2.1	53.2 (52.6)±2.1	60	52.5(50.8)±2.1	47.1(45.2)±2.0
4.0	56.8(56.2)±2.1	55.1 (54.5)±2.0	70	48.6(47.0)±1.8	45.6(43.8)±2.0
4.5	60.7(60.0)±2.3	57.4 (56.7)±2.2	80	45.4(43.8)±1.8	42.4(40.7)±1.9
5.0	68.9(68.1)±2.5	58.3(57.5)±2.4	90	44.2(42.8)±2.0	41.1(39.6)±1.8
5.5	72.5(71.6)±2.7	60.9(60.1)±2.6	100	41.3(40.0)±1.6	38.8(37.4)±1.6
6.0	77.3(76.5)±2.8	69.2(68.2)±2.6	120	38.5(37.3)±1.3	36.3(35.0)±1.2
6.5	80.5(79.5)±3.0	69.2(68.2)±2.7	150	34.3(33.3)±1.2	32.3(31.1)±1.1
7.0	81.9(80.7)±3.0	71.2(71.1)±2.7	200	30.3(29.4)±1.0	28.0(27.1)±0.9
7.5	81.4(80.1)±3.1	69.1(67.8)±2.7	250	27.1(26.4)±0.9	24.8(24.0)±0.9
8.0	81.6(80.4)±3.0	70.1(68.8)±2.6	300	24.4(23.8)±0.8	22.1(21.5)±0.8
8.5	81.3(80.0)±3.1	68.8(67.2)±2.7	400	20.5(20.0)±0.7	19.1(18.5)±0.6
9.0	80.3(78.9)±2.9	68.1(66.5)±2.6	500	18.2(17.8)±0.6	16.7(16.3)±0.6
9.5	80.1(78.7)±3.0	66.8(65.2)±2.6	600	16.1(15.8)±0.5	14.6(14.2)±0.5
10	78.7(77.3)±2.8	65.9(64.3)±2.5	800	11.5(11.3)±0.4	11.4(11.1)±0.3
11	75.9(74.3)±2.7	61.8(60.1)±2.3	1000	9.3(9.1)±0.3	10.3(10.1)±0.3
12	74.3(72.6)±2.8	60.4(58.7)±2.3			

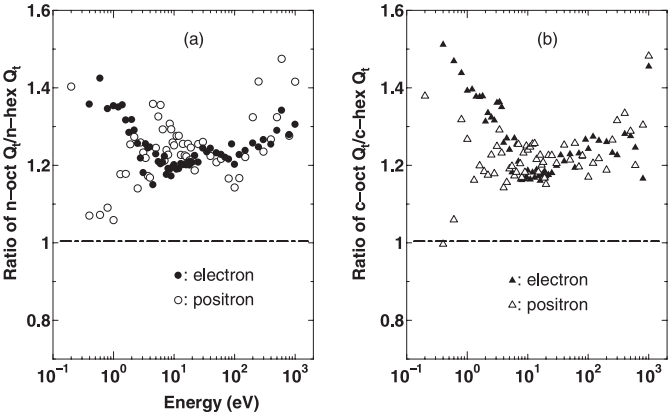

Fig. 5. TCS ratios for (a) n-octane/n-hexane for electron and positron impact; (b) c-octane/c-hexane for electron and positron impact.

plotted in Figure 5. The data in Figures 4a and 4b show that both n- and c-octane TCSs are greater than their corresponding n- and c-hexane TCSs over all the energy ranges. This is the molecular size effect that has been observed in both positron and electron scattering for a number of molecules we have studied before (e.g. see Ref. [10]). This is an effect whereby when molecules become larger in geometrical size, accordingly, the electron charge distribution is likely to spread out spatially increasing scattering events. As a general rule, the larger the molecular size the larger the TCS tends to be. It also worth noting that a great deal of similarities in shape and magnitude of the curves for these ratios for both positron and electron scattering, which is very interesting. For positron scattering, a peak feature is observed at 4–10 eV in Figure 5a. We took interest in examining this feature by carrying out separate measurements, albeit using a novel method, and determined the positronium (Ps) formation in these molecules at 2 eV above their respective Ps formation threshold energies, E_{Ps}, i.e. 3.4 eV and 3.38 eV for n-octane and n-hexane, respectively. The result was that the contribution of the Ps formation cross-section to the TCS was ∼5.8% in the former and ∼8.9% in the latter [21]. Thus, though these are only values 2 eV above E_{Ps}, we speculate that this peak feature should possibly be due to some TCS enhancement, stronger in n-octane than n-hexane, due to rovibrational and/or electronic

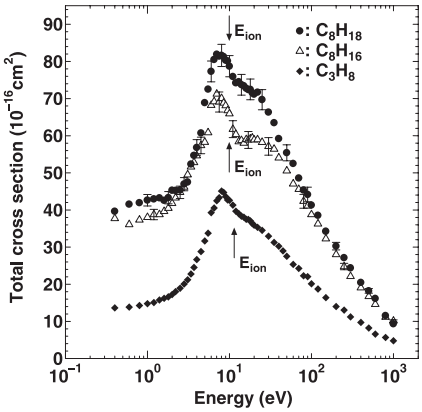

Fig. 6. Total cross-sections for electron scattering from n-octane, c-octane and propane molecules. Arrows indicate thresholds of Ps formation, $E_{\rm Ps}$, and ionization, E_{ion}.

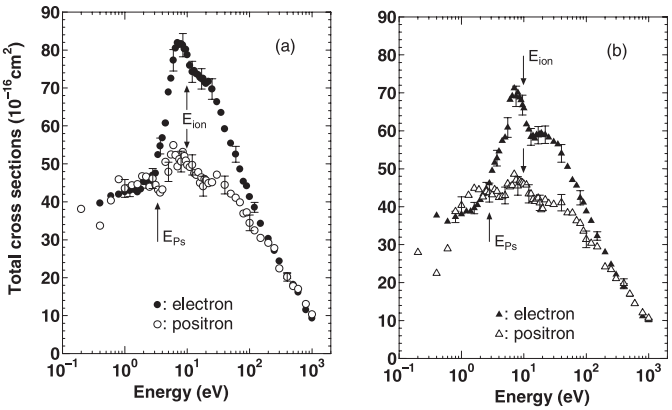

Fig. 7. Positron TCSs for (a) n-octane and (b) c-octane molecules. Arrows indicate thresholds of Ps formation, $E_{\rm Ps}$, and ionization, E_{ion}.

excitation. It would also be interesting to know if the rather less known positron dissociative attachment could be involved in this feature. Otherwise, for Figures 5a and 5b, ratios for positron TCSs show a rather similar behavior at 2 eV to 300 eV, both having an average magnitude of about 1.23, pointing to the difference in the molecular size. However, both decrease to a minimum with decreasing energy below 4 eV. Both also rise with increasing energy above 300 eV. For electron scattering on the other hand, both ratios (in Figs. 5a and 5b) are rising monotonously below 3 eV. However, like the positron case, they produce a broad plateau at 2–300 eV, before rising too with increasing energy above 300 eV. These similarities point not only to the similarity between the individual pairs of normal molecules and cyclo molecules, but also to the fact that all four molecules exhibit some similarity in their TCSs for positron and electron scattering. That the curves for both positron and electron TCSs are not flat across the whole energy range points to the differences in the energy dependence of the individual TCSs, i.e. with different structures being observed at different energies. Peaks in these ratio curves indicate peaks in the octane TCSs in energy regions where hexane TCSs do not show strong enhancements, and vice versa.

3.2 Electron scattering

The TCSs for electron scattering from n- and c-octane are shown in Figure 6, in comparison with those for n-propane molecules. These two molecules are isomers having different molecular structures i.e. a linear structure for C_8H_{18},and a ring shape for cyclo-C_8H_{16} molecules and different numbers of H atoms. In a way similar to other alkanes and hydrocarbons, TCSs for both molecules show two shape-resonance peaks, a relatively sharp one at about 8 eV and a broader but weaker one at around 15–25 eV. The 8 eV peak has been attributed to a shape resonance arising from an unoccupied π orbital, while the small structures clustered at 15–25 eV are due to a combination of shape resonances of higher symmetries. These TCSs decrease sharply at the lower energy side of the 8 eV peak. C_8H_{18}TCSs are greater than cyclo-C_8H_{16}TCSs at all energies, being about 20% greater at 8 eV, for instance. Above 50 eV, the decrease is rather gradual for both molecules. That C_8H_{18}TCSs are greater than cyclo-C_8H_{16} TCSs, even above a few hundred eV, is a clear reflection of the molecular size effect i.e. the greater the molecular size the greater the TCS magnitude.

3.3 Positron and electron scattering

The TCSs for positron and electron scattering are shown in Figure 7a for n-octane and 7b for c-octane molecules. Interestingly, positron TCSs for both molecules become higher than electron TCSs at 0.8–2.5 eV, although electron TCSs still fall within the error bars of the positron TCS data. However, this trend is quickly reversed as electron TCSs seem to have already become larger than positron TCSs below 0.6 eV and above 3.0 eV. It is also interesting to note that, for both molecules, the electron and positron TCS peaks appear centered at the same energy position of about 8 eV, though the positron peak is broader. We speculate the reason why this peak is narrower in electron than positron TCSs to be the presence of long-lived shape resonance enhancements in electron impact but not in the latter. This peak position feature seems to be the same also for C_3H_8, C_5H_{12} and C_6H_{14} molecules [5], but is surely not so for CH_4 and C_2H_6 where there is a shift to higher energies for positron TCSs than electron TCSs. Merging of the electron and positron TCSs for both molecules occurs, i.e. above 200 eV for n-octane and 250 eV for c-octane. It is interesting to note that the merging energy varies from system to system so drastically, i.e. for n-propane (C_3H_8) and larger molecules, in this alkane family.

3.4 Comparison between TCSs for normal- and cyclo-octane

We are also interested in the comparative study of the positron and electron scattering in normal-molecules with

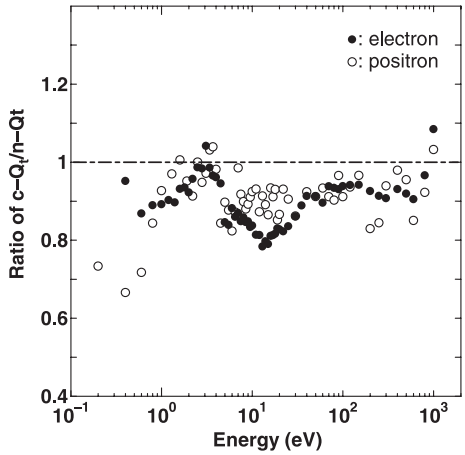

Fig. 8. Ratios of TCSs of c-octane to those of n-octane for positron and electron scattering.

those in the cyclo-molecules. For this study, the ratios of the c-octane/n-octane electron TCSs are plotted together with the ratios for positron scattering in Figure 8. It is interesting to note from this figure that, except for the 5–40 eV energy range, the ratio curves for electron and positron scattering are similar in both energy dependence and magnitudes. Peaks in these ratio curves indicate peaks in the c-octane TCSs in energy regions where n-octane TCSs do not show strong enhancements, and vice versa. Comparing the octane data shown in Figure 8 with the similar data for hexane [7], the main difference is at 1.3–6 eV, where the positron ratios are comparable to the electron data, whereas for hexane the electron data is smaller than the positron data over the same energy range.

4 Conclusion

Total cross-sections for n-octane and c-octane molecules have been investigated for 0.2–1000 eV positron and 0.4–1000 eV electron impact as part of the systematic study being carried out for the alkane family of molecules. For positron scattering, both TCSs show a peak at 1.5–2.5 eV, a feature that is observed for all alkanes from C_3H_8 and larger. The magnitudes of the n-octane TCSs are greater than those for c-octane over all the energy range studied. In the comparative study between positron and electron TCSs, positron TCSs for both molecules become higher than electron TCSs at 0.8–2.5 eV. Merging of the electron and positron TCSs for both molecules occurs, i.e. above 200 eV for n-octane and 250 eV for c-octane. Similarities with our previous study of n- and c-hexane have been observed.

The authors acknowledge Dr. A. Hamada for the measurements in the earlier stage. This work was partly supported by the Grand-in-Aid, the Ministry of Education, Science, Technology and Culture, Japan. Authors CM and MK are also grateful to the Japan Society for the Promotion of Science (JSPS) for financial support under the grant number P04064, and also to Yamaguchi University where CM did part of this work whilst he was a Ph.D. student there.

References

1. W.L. Morgan, Adv. At. Mol. Opt. Phys. **43**, 79 (2000)
2. Y. Hatano, Adv. At. Mol. Opt. Phys. **43**, 231 (2002)
3. T.M. Miller, J.F. Friedman, A.A. Viggiano, J. Chem. Phys. **120**, 7024 (2004)
4. M. Jelisavic, R. Panajotovic, M. Kitajima, M. Hoshino, H. Tanaka, S.J. Buckman, J. Chem. Phys. **121**, 5272 (2004)
5. M. Kimura, O. Sueoka, A. Hamada, Y. Itikawa, Adv. Chem. Phys. **111**, 537 (1999)
6. O. Sueoka, M. Kawada, A. Hamada, H. Tanaka, M. Kitajima, M. Kimura, In *International Symposium on Electron- Molecules Collisions and Swarms*, Tokyo, Japan, July 1999, pp. 195
7. O. Sueoka, C. Makochekanwa, H. Tanino, M. Kimura, Phys. Rev. A **72**, 042705 (2005)
8. C.M. Surko, G.F. Gribakin, S.J. Buckman, J. Phys. B **38**, R57 (2005)
9. A. Hamada, O. Sueoka, J. Phys. B **27**, 5055 (1994)
10. O. Sueoka, C. Makochekanwa, H. Kawate, Nucl. Instr. Meth. B **192**, 206 (2002)
11. L.G. Christophorou, M.W. Grant, D. Pittman, Chem. Phys. Lett. **38**, 100 (1976)
12. O. Sueoka, S. Mori, A. Hamada, J. Phys. B **27**, 1453 (1994)
13. O. Sueoka, S. Mori, J. Phys. B **19**, 4035 (1986)
14. M. Kimura, C. Makochekanwa, O. Sueoka, J. Phys. B **37**, 1461 (2004)
15. K.R. Hoffman, M.S. Dababneh, Y.-F. Hsieh, W.E. Kauppila, V. Pol, J.H. Smart, T.S. Stein, Phys. Rev. A **25**, 1393 (1982)
16. P.G. Coleman, T.C. Griffith, G.R. Hyland, Appl. Phys. **5**, 223 (1974)
17. L. Boesten, H. Tanaka, J. Phys. B **24**, 821 (1991)
18. H. Tanaka, L. Boesten, D. Matsunaga, T. Kudo, J. Phys. B **21**, 1255 (1988)
19. L. Boesten, M.A. Dillon, H. Tanaka, M. Kimura, H. Sato, J. Phys. B **27**, 1845 (1994)
20. C. Makochekanwa, H. Kato, M. Hoshino, H. Tanaka, H. Kubo, M.H.F. Bettega, A.R. Lopes, M.A.P. Lima, L.G. Ferreira, J. Chem. Phys. (in press)
21. C. Makochekanwa, O. Sueoka, M. Kimura, Nucl. Instr. Meth. B (submitted)